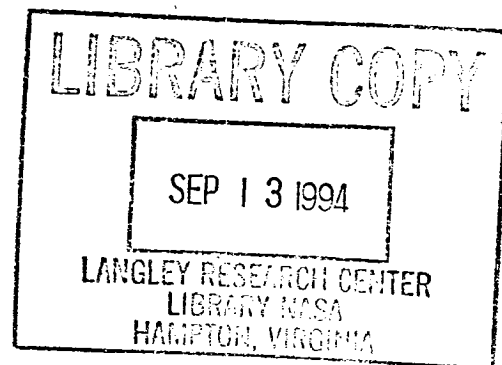


# **NASA ER-2 Doppler Radar Reflectivity Calibration for the CAMEX Project**

**I. J. Caylor, G. M. Heymsfield, S. W. Bidwell, and S. Ameen**

**AUGUST 1994**





**NASA Technical Memorandum 104611**

**NASA ER-2 Doppler Radar  
Reflectivity Calibration for the  
CAMEX Project**

**I. J. Caylor  
S. Ameen**  
*Science Systems and Applications, Inc.  
Lanham, Maryland*

**G. M. Heymsfield  
S. W. Bidwell**  
*Goddard Space Flight Center  
Greenbelt, Maryland*



National Aeronautics and  
Space Administration

**Goddard Space Flight Center**  
Greenbelt, Maryland 20771  
1994

This publication is available from the NASA Center for Aerospace Information,  
800 Elkridge Landing Road, Linthicum Heights, MD 21090-2934, (301) 621-0390.

## Table of Contents

	Page
1. Introduction . . . . .	1
2. EDOP Hardware . . . . .	1
3. Receiver Calibration . . . . .	3
3.1 Receiver Losses . . . . .	4
3.2 External Source Calibration . . . . .	4
3.3 Internal Source Calibration . . . . .	5
4. Antenna Gain . . . . .	6
5. Transmitted Power . . . . .	7
6. Radar Constants . . . . .	7
7. Long-Term Stability . . . . .	9
8. Range Equation . . . . .	10
9. Ground Truth Comparison . . . . .	11
9.1 WSR-88D Processing . . . . .	11
9.2 EDOP Processing . . . . .	12
9.3 Comparison of EDOP and WSR-88D . . . . .	12
10. Ocean Surface Analysis . . . . .	13
11. Forward Beam . . . . .	14
12. Summary . . . . .	14
13. References . . . . .	15



## 1. INTRODUCTION

The NASA ER-2 Doppler radar (EDOP) participated in the Convection and Atmospheric Moisture Experiment (CAMEX) based at the Wallops Flight Facility during September and October 1993. The data obtained during these flights represent the first reliable reflectivity measurements from the EDOP instrument. This report describes the calibration of the CAMEX reflectivity data.

Because the configuration of the EDOP microwave and signal processing systems has been altered since the conclusion of CAMEX, the calibrations presented in this report should not be considered definitive in terms of future campaigns. However, the calibration procedure as described can be adapted easily.

The weather radar equation relates radar hardware characteristics and received power to a physically meaningful parameter called the effective reflectivity factor ( $Z_e$ ). The equation is

$$Z_e = R^2 P_r \left[ \frac{\lambda^2 l_r}{P_t G^2 \phi^2 k^2} \frac{1024 \ln 2}{c \tau \pi^3} \right], \quad (1)$$

where the quantity in brackets is termed the radar constant and contains the radar system parameters. These parameters are the wavelength ( $\lambda$ ), the antenna gain ( $G$ ), the beamwidth ( $\phi$ ), the pulse width ( $\tau$ ), receiver system losses ( $l_r$ ), and a dielectric constant for water,  $|k|^2 \approx 0.93$ . The peak transmit power is ( $P_t$ ), the received power ( $P_r$ ), and range ( $R$ ).

Therefore, the radar equation can be rewritten in logarithmic units as

$$\text{dBZ}_e = RC[\text{dB}] + P_r[\text{dBm}] + 20 \log(R), \quad (2)$$

where  $RC$  is the radar constant in units of decibels (dB) and contains the hardware-dependent parameters. A receiver calibration is used to convert the power ( $P_r$ ) from measured engineering units (A/D counts) into dBm. These values, along with a range vector (gate spacing), can be used to compute dBZ from Equation 2. Zero dBZ is the reflectivity factor in dB for a 1-mm diameter drop per cubic meter.

The primary purpose of this report is to evaluate the three terms in Equation 2. In the following sections, the EDOP radar will be briefly described followed by discussions pertaining to each of the primary terms in Equation 1:  $P_t$ ,  $P_r$ , the antenna gain ( $G$ ), and the losses

( $l_r$ ). Using these results, the radar constants are computed for each of the EDOP receivers.

Data obtained during the CAMEX flight on 5 October 1993 are used to illustrate the results of the calibration analysis for precipitation echoes. In particular, the calibrated reflectivity is compared with data from a ground-based radar, and the scattering cross section for the ocean surface is also estimated. The ranging performance is evaluated, as is the long-term stability of the radar hardware. A summary, along with recommendations for calibrations in future field campaigns, is contained in the final section.

Drs. Lee Miller and Robert Meneghini are thanked for their many helpful comments and discussions. Mr. Marshall Shepherd acquired the weather buoy and Melbourne WSR-88D data and the authors appreciate his diligent efforts installing the WSR-88D formatting software.

## 2. EDOP HARDWARE

This section is not intended to be a comprehensive discussion of the EDOP hardware but rather a brief description of hardware related to calibration issues. Additional details of the radar hardware and software can be found in NASA documentation and overviews by Heymsfield *et al.* (1989, 1991, 1993).

EDOP is a dual antenna X band multiparameter radar housed in the nose of the NASA ER-2 high-altitude aircraft. One antenna is fixed in the nadir direction, while the forward antenna is oriented to stare along the aircraft flight track  $30^\circ$  forward of nadir. Table 1 lists the primary EDOP specifications. Note that although the hardware for Doppler measurements was in place during CAMEX, the Doppler parameters were not provided by the real-time data system.

A block diagram of the transmitter and receiver is shown in Figure 1. The two antennas share a coherent transmitter, the power being divided equally, as well as the associated oscillator and timing components. The nadir receiver detects vertically polarized copolar (VV) returns while the forward receiver is a dual channel system that can simultaneously process the vertical copolar (VV) and cross-polar (VH) returned powers. Thus, there are three logarithmic receiver chains from two antennas which require calibration. Although only reflectivity processing was available for CAMEX, the Doppler signal processor software is implemented at Goddard Space Flight Center.



TABLE 1. EDOP Radar Specifications

<b>Transmitter</b>	
Frequency	9.72 GHz
Peak Power (nominal)	25 kw
Duty Cycle	0.0044 max.
Pulse Width	0.25, 0.5, 1.0 $\mu$ s
PRF	2200, 4400 Hz
<b>Antenna</b>	
Antennas	2
Antenna Diameter	0.76 m
Antenna Beamwidth	2.9°
Type	Offset paraboloid
Gain (nominal)	36 dB
First Sidelobe Level	< -26 dB
Cross-polarization Level	< -30 dB
Transmit Polarization	
Nadir	Vertical
Forward	Vertical
Receive Polarization	
Nadir	Copolar
Forward	Co and cross-polar
<b>Receiver</b>	
Noise Figure	1.79 dB
Intermediate Frequency	60 MHz
Linear Doppler Channels	2
Log Reflectivity Channels	3
Dynamic Range with AGC	110 dB
<b>Data System</b>	
A/D Converters	7x12 bits, 10 MHz
Signal Processors	24xAT&T DSP32C
Gate Spacing	150, 75, 37.5 m
Gates	872 (max)
Integration Cycle	0.25 to 1.0 s
Products	
Nadir	Z, $\nu$ , $\sigma$ , SNR
Forward	Z, LDR, $\nu$ , $\sigma$ , SNR

Figure 1 illustrates several features that are relevant to the EDOP calibration. EDOP contains an internal calibration system routes a continuous wave (CW) signal into the receiver. In addition, the receiver and transmitter chassis are physically separated in the nose of the ER-2 and are connected by lengths of semirigid coax cable which have a significant loss.

Although a standard target sphere calibration is highly desirable, the physical arrangement of EDOP poses problems for such a calibration. The microwave and

data systems, along with the antennas, are fixed into the ER-2 nose structure pointing downwards through a radome. In addition, the antennas are nonsteerable. Therefore, performing an end-to-end calibration on an external target with the system installed in flight configuration is rather impractical.

There are a number of operating parameters which can be configured at flight time.

- Pulse repetition frequency (PRF)
- Transmitted pulse width ( $\tau$ )
- IF bandwidth
- Integration cycle
- Sampling frequency and number of gates

These parameters, which may vary from flight to flight, depending on observational objectives, must be accounted for in order to properly calibrate the received power into effective reflectivity factor.

In addition, the radar signal processor can operate in one of two modes. One mode, termed *raw*, provides a subset of the time series at each gate, typically 16 independent samples per second. The second processor configuration is termed *processed* mode in which the complete time series are integrated in real time at each gate over a specified time interval (typical integration cycles are 0.5 and 1.0 s). Since the averaging is done with samples from a logarithmic amplifier, a bias is introduced in the estimated mean. This bias depends on the number of independent samples and, hence, the integration mode of the processor.

### 3. RECEIVER CALIBRATION

No rigorous calibration was performed prior to CAMEX, but upon the completion of the experiment, the radar was removed from the ER-2 nose and set up at Goddard Space Flight Center (GSFC). The GSFC configuration does not include the antennas and involves a different set of waveguide and connecting radio frequency (RF) cables. As will be explained later, this requires some correction to the resulting receiver calibration in order to be applicable to the data recorded during CAMEX flights.

A receiver calibration is used to convert the returned echo power ( $P_r$ ) from engineering units into units of power through a function called the calibration curve. In general, the engineering units are binary A/D counts, while power is expressed logarithmically as

dBm. Although the digitizer counts ( $C_D$ ) are directly related to the power collected by the antenna, there are gains, losses and nonlinearities in the receiver chain which must be taken into account.

Received power ( $P_r$ ) is estimated by adding the receiver loss ( $l_r$ ) to the power measured at each calibration step ( $P_m$ ), in units of dB:

$$P_r = P_m(C_D) + l_r, \quad (3)$$

where  $P_m$  is a function of the digital counts.

### 3.1 Receiver Losses

Received power is the echo power present at the antenna port and can be estimated by using the calibration curve and accounting for losses associated within the receiver itself. These losses can be divided into two general groups. Losses which are constant, such as waveguide and insertion losses, can be termed *fixed* losses. Losses which depend on the variable flight configuration of the radar and data processing (Section 2), such as length of integration and IF bandwidth, are termed *configuration* losses. It should be noted that configuration losses are constant for any given flight.

The receiver loss for EDOP is divided into three components. There is a fixed loss ( $l_g$ ) associated with the radome and waveguide. A second term gives the difference between the insertion loss of the IF filter ( $\Delta l_i$ ) used in flight and that used for the calibration. The third component is a loss, or more accurately a correction factor,  $\Delta l_c$ , for differences between laboratory and flight configurations in the semirigid RF cable connecting the transmitter and receiver enclosures.

$$P_r = P_m + l_g + \Delta l_i + \Delta l_c. \quad (4)$$

The fixed and variable losses are listed in Tables 2 and 3, respectively. It should be noted that the above values do not include the logarithmic integration bias which will be accounted for in the final computation of the radar constant.

In general, the fixed losses are those specified by the manufacturer and are assumed to be accurate. The waveguide loss listed in Table 2 was measured by personnel at the NASA Wallops Flight Facility.

The radome loss is a theoretical estimate for an A-sandwich material with the dimensions as used in the

ER-2 nose (Dicaudo, 1970). The radome loss estimate assumes a normal incidence angle against a plane radome surface. This is approximately the case for the nadir beam, while the loss for the forward beam may be slightly higher than listed in Table 2 because of the more complicated geometry of the radome.

The IF filter insertion loss only needs to be considered for the case where the calibration measurements were performed with a filter different from that used to acquire reflectivity data. In such a case, only the differential insertion loss between the two filters should be used in Equation 4 (see Table 9).

TABLE 2. EDOP Receiver Fixed Losses ( $l_g$ )

	Nadir	Forward VV	Forward VH
Radome	0.11	0.11	0.18
Rotary joint	0.1	N/A	N/A
Waveguide	0.15	0.30	0.24
T/R circulator	0.2	0.2	0.2

TABLE 3. Correction ( $l_c$ ) for EDOP RF Cables for External Calibration

	Nadir	Forward VV	Forward VH
Flight cables	3.55	3.17	3.41
Bench cables	1.00	1.00	1.00
Correction	2.55	2.17	2.41

### 3.2 External Source Calibration

A typical technique to calibrate the receiver chain is to insert a known pulsed radio frequency (RF) power level at the top of the chain in the best case at the antenna port. The RF power is stepped through a number of levels covering the receiver's dynamic range while the resulting A/D binary count values are recorded. In this manner, a function can be

determined which relates A/D counts to dBm. This procedure effectively incorporates most, if not all, of the gains and losses inherent in the receiver system.

A vector network analyzer (Hewlett Packard 8510C) was used to inject a single frequency RF pulse ( $\tau=2 \mu\text{s}$ ) into the nadir antenna port. The analyzer was stepped through the dynamic range of the receiver front-end low-noise amplifier, from approximately 0 to -110 dBm by increments of 5 dBm. Separate tests were also performed for the forward copolar and cross-polar receivers.

The total receiver loss for each of the three channels was computed from Tables 2 and 3 using Equation 4.

Nadir VV Loss:	2.21 dB
Forward VV Loss:	1.78 dB
Forward VH Loss:	2.43 dB

In this case,  $\Delta I_i$  is not zero and is given by the insertion loss difference between the 8-MHz and 2-MHz filters (see Table 9). The circulator insertion loss is neglected, since it is in the calibration path.

Using the receiver losses and calibration test data, the received power can be estimated from Equation 3. The results of the calibration for the three receivers is shown in Figure 2. It is clear that there is saturation at the top of the dynamic range at approximately -20 dBm. The maximum count level of 2047 is attained by the nadir channel, so it is likely that the

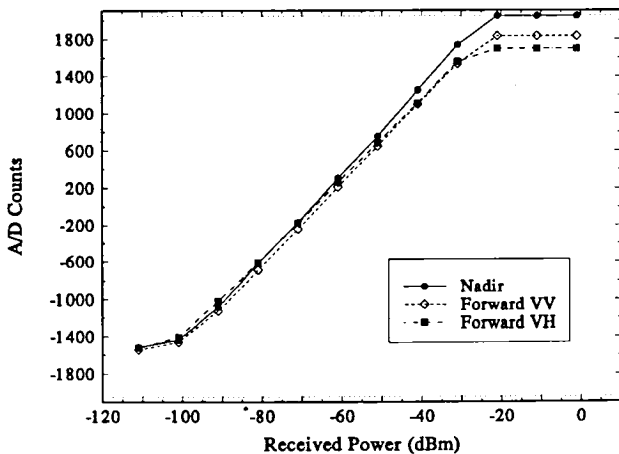


FIGURE 2. Results of the three channel receiver calibration using an external pulsed RF source.

A/D itself is saturating. However, the two forward channels saturate at lower count values, which indicates that the amplifiers on the signal conditioning card are being saturated.

### 3.3 Internal Source Calibration

EDOP provides an internal calibration chain so that performance of the radar can be tracked during flight. The RF calibration source is a continuous wave (CW) signal from the field-effect transistor amplifier in the travelling wave tube (TWT) exciter (see Figure 1). During calibration, the exciter signal is routed from the TWT with a directional coupler into a series of variable attenuators located in the transmitter chassis. The attenuator output is split with a 4-way power divider to feed the three receiver chains via PIN diode switches just after the transmit/receive circulators. During laboratory tests, a self-calibrating power meter (Hewlett Packard 437B) was connected to the fourth port of the power splitter to monitor the absolute calibration power level.

It is important to note that losses after the switches are folded into the calibration curve, whereas losses ahead of the switches, and hence not part of the calibration path, must be explicitly accounted for in the analysis.

There are two straightforward methods to measure the power at each attenuator setting. If the attenuation at a given setting is well known, then the input power to the attenuator can be measured once and the value at each step computed from the attenuation. The second method involves measuring the output power directly from the attenuator at each step; in which case, knowledge of the attenuation value at each setting is not required. Because of limitations on the dynamic range of the power meter, the first method was selected for use with EDOP calibration.

The EDOP radar uses a pair of 6-bit digitally programmable RF attenuators in series which can provide nominal attenuation from 0 to 126 dB. The specification for the digital attenuator indicates that the deviation from the digital setting is proportional ( $\pm 3\%$ ) to the attenuation, and so the actual attenuation can vary significantly from that which is selected. In order to provide a greater accuracy during calibration, the attenuation for each of the two units was measured and is listed in Table 4. Attenuator B is generally within the manufacturer's specification, while the values for attenuator A deviate quite significantly (19.4%).

For the calibration measurement at GSFC, short lengths (approximately 2.25 ft) of semirigid coax were used to connect the transmitter to the receiver, while the length of the cables used for flight operations is about 7.25 ft. The transmission loss of a 0.141-inch-diameter semirigid coax is approximately 0.38 dB ft<sup>-1</sup> at a frequency of 9.72 GHz. There is an additional attenuation which is attributed to the SMA connectors. The measured attenuation for the flight cables and the estimated attenuation for the cables used on the bench are listed in Table 5 and the difference between these two values is the correction factor ( $\Delta l_c$ ) in Equation 4.

Summing the losses in Tables 2 and 5 gives the total receiver loss ( $l_r$ ) for each channel.

Nadir VV Loss:	2.63 dB
Forward VV Loss:	2.30 dB
Forward VH Loss:	2.55 dB

For the internal calibration, the bandpass filter is identical to that used in flight so  $\Delta l_c = 0$ .

The resulting calibration curves from the internal calibration test are shown in Figure 3. These curves have very similar slopes to the curves in Figure 2 and also saturate in a similar manner. However, there are some obvious nonlinearities which are attributed to instability of the digital attenuators.

#### 4. ANTENNA GAIN

The antennas used for EDOP are of an offset paraboloid type. The manufacturer's measured gains for the antennas are

Nadir VV Gain:	36.1 dB
Forward VV Gain:	36.3 dB
Forward VH Gain:	36.4 dB

at a frequency of 9.625 GHz (Davis, 1991). The beam widths are approximately 2.9° in both the E and H planes.

A fact that is not accounted for is that the center frequency for EDOP is actually 9.72 GHz, which may change the gains listed above because of the narrow

TABLE 4. Measured Attenuations for the EDOP Digital Attenuators

Setting (dB)	Attenuator A	Attenuator B
1	0.93	0.61
2	1.79	1.74
4	3.87	4.00
8	6.76	8.16
16	13.41	16.11
32	25.78	31.17
63	52.54	61.79

TABLE 5. Correction ( $l_c$ ) for EDOP RF Cables for Internal Calibration

	Nadir	Forward VV	Forward VH
Flight cables	3.55	3.17	3.41
Bench cables	1.48	1.48	1.48
Correction	2.07	1.69	1.93

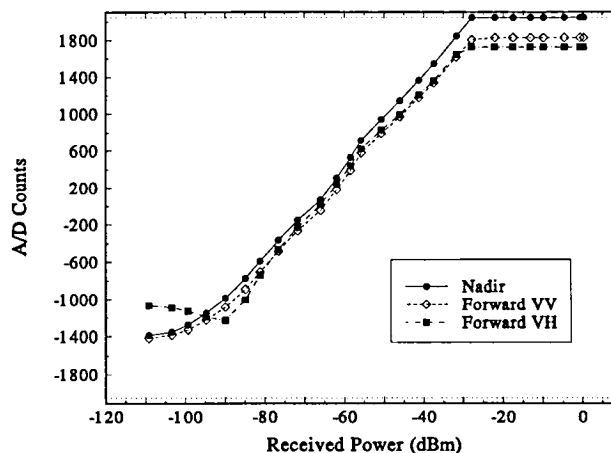


FIGURE 3. Three channel receiver calibration using the internal CW calibration source.

design bandwidth of the antennas. However, it is believed that any deviations are small.

Unfortunately, because of complications which arose during initial installation into the ER-2, the forward antenna was moved out of focus. While realignment of the forward antenna has subsequently been completed, the above antenna gains will be used for the CAMEX calibration. Adjustment of the radar constant for the forward beam is discussed in Section 11.

## 5. TRANSMITTED POWER

The peak transmitted power for the forward and nadir channels were measured at GSFC.

Nadir:	68.0 dBm
Forward:	68.1 dBm

The measurement was made at the output port of the transmitter chassis and includes losses for an arc detector, 50-dB coupler, and power splitter. However, in the flight configuration, there are a number of further losses which reduce the transmitted power as shown in Table 6. Note that the waveguide loss ( $l_g$ ) from Table 2 is also listed since the same antenna is used for transmission and reception.

The transmitted power is found by subtracting the losses in Table 6 from the measured value for the peak power.

TABLE 6. Losses ( $l_g$ ) for EDOP Transmit Power

	Nadir	Forward
Waveguide	0.15	0.30
Rotary joint	0.1	0.1
Radome	0.11	0.11
Total	0.36	0.41

## 6. RADAR CONSTANTS

Four flights were achieved during the CAMEX project, and the radar configuration for each is shown in Table 7. On the first flight only qualitative data were obtained because of a faulty power regulator on the signal conditioning card. The regulator was replaced and, for the remaining three flights, the processor was configured to operate in raw mode with an acquisition time of one sample per range gate every 0.06 s. The radar constants will be computed for the configuration of the final three flights.

The radar constant, in units of dB, is given by

$$RC = 169.14 + l_{int} + l_{bw} - 2G - (P_r - l_g) + 10 \log \left( \frac{\lambda^2}{\phi^2 \tau} \right), \quad (5)$$

The first four terms are in units of dB and, for the CAMEX flights, the last term of Equation 5 evaluates to 61.44 dB ( $\tau=0.25\mu s$ ). The effective reflectivity factor is defined with units of  $mm^6 \cdot m^{-3}$ , and the range is usually defined in units of kilometers. These two unit conversions introduce an additional factor of 240 dB ( $10^{24}$ ) in the radar constant.

The integration loss is a numerical effect caused by integrating the received signal in logarithmic units (dB) rather than linear units (mW) where the mean of a sum of logarithmic values is biased from the true mean. For randomly varying radar signals, the bias is a function of the number of independent samples used in the average (Zrnice, 1975). As the number of independent samples increases to about 32, the bias rapidly approaches a limit of 2.5 dB (Table 8). At an interval of 0.06 s, each sample is effectively independent, and, if 32 or more samples are used to compute the mean power, then  $l_{int} = 2.5$  dB.

The loss related to the IF filter bandwidth is described by Doviak and Zrnice (1979). This loss results from distortion of the received pulse by the IF bandpass filter. Therefore, this loss factor can vary for EDOP, depending on the width of the transmitted pulse and the width of the selected IF filter (2 or 8 MHz). Table 9 lists losses for the four possible combinations of pulse width and IF filter bandwidth and for the CAMEX flights  $l_{bw} = 3.99$  dB.

The EDOP radar constants for the CAMEX project are computed from Equation 5 and shown below. Note that for the forward VH (cross-polar) channel, the

TABLE 7. EDOP Configuration for CAMEX

	12 September	25 September	3 October	5 October
Mode	Processed	Raw	Raw	Raw
Pulse width ( $\mu\text{s}$ )	0.25	0.25	0.25	0.25
IF bandwidth (MHz)	2.0	2.0	2.0	2.0
PRF (Hz)	2200	2200	2200	2200
Gate spacing (m)	75	150	150	150
Integration (s)	1.0	N/A	N/A	N/A
Sample interval (s)	N/A	0.06	0.06	0.06

TABLE 8. EDOP Losses ( $l_{int}$ ) for Logarithmic Integration Bias

Independent Samples	Integration Bias (dB)
8	2.1
16	2.3
>32	2.5

TABLE 9. EDOP Losses ( $l_{bw}$  and  $l_i$ ) for IF Filter Bandwidth

3dB Bandwidth (MHz)	Filter Loss, $l_{bw}$ (dB)		Insertion Loss, $l_i$ (dB)		
	$\tau=0.25\mu\text{s}$	$\tau=1.0\mu\text{s}$	Nadir	Forward VV	Forward VH
2.0	3.99	0.90	4.6	4.6	5.0
8.0	0.90	0.21	5.3	5.4	5.4

factor of 2G is actually the vertical copolar gain times the cross-polar gain (Section 4).

Nadir VV:	97.51 dB
Forward VV:	97.06 dB
Forward VH:	96.96 dB

## 7. LONG-TERM STABILITY

The long-term stability of EDOP, particularly in relation to thermal conditions, was investigated by examining two parameters extracted from the flight data of 5 October 1993: the receiver background noise level and the peak level of the transmitted pulse.

The high power transmitted pulse, although significantly attenuated, leaks through a circulator and a T/R switch into the receiver. Since the data system begins digitizing prior to each PRT, the transmitted pulse is sampled, in a qualitative manner, at all times throughout the flight. Figure 4 shows the transmitted pulse peak level for the three receivers over a period of approximately 2.5 hours. After an initial period for the radar to reach equilibrium temperature, the leakage level is very constant to better than 0.25 dB.

The receiver background noise level was computed by averaging data from range gates in which no cloud echo appeared. The gates selected for this analysis were those approximately 0.825 to 1.05 km below the ER-2, which was above cloud top for the 5 October 1993 flight. An analysis which produced similar results was also performed for gates well beyond the surface echo.

The background noise level (Figure 5) shows several short-term excursions of about 2 dB. Analysis of surface return echoes shows these excursions are associated with passage of the ER-2 over water rather than land. The NASA AMPR 10-GHz radiometer data were examined, and the excursions in the radar background level are highly correlated with deviations of  $>100^\circ$  K in the brightness temperature. In terms of radar stability, however, the noise level exhibits no long-term trends over the course of the flight.

The signal processor was programmed to make periodic internal calibrations (Section 3.3) during the 5 October 1993 flight. During the calibration, an attenuator was stepped through a range of settings.

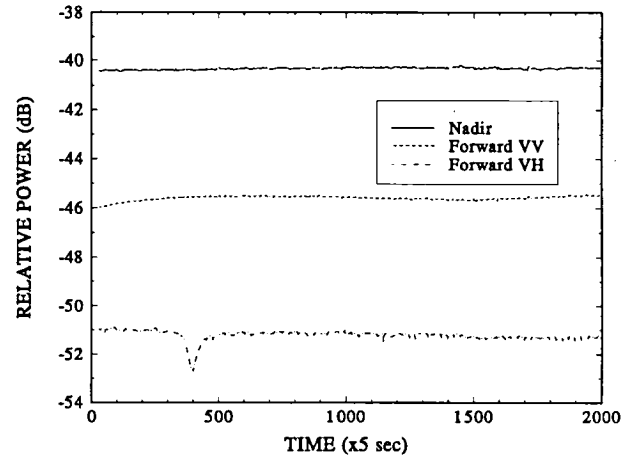


FIGURE 4. Peak value of the transmit pulse for the nadir (solid), forward copolar (dashed) and cross-polar (dot-dash) receivers.

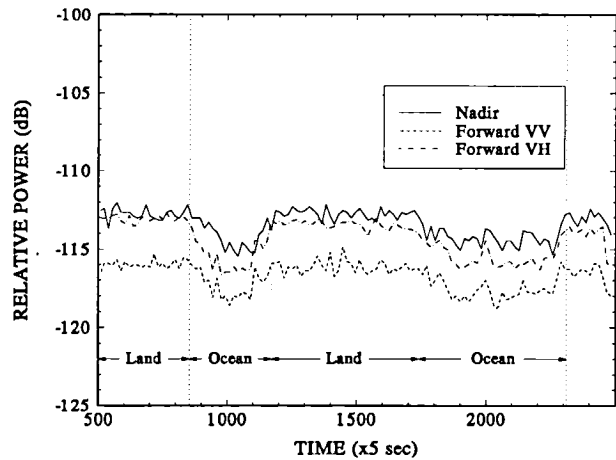


FIGURE 5. Background noise level for the three receivers, as in Figure 4.

Data from each calibration performed during flight was extracted for the 63-dB setting. These data (Figure 6) show a large and long-term trend of over 1 dB during the course of the flight, while data at a higher attenuation setting of 95 dB exhibit a long-term drift of nearly 5 dB (see Figure 7).

The above results indicate that the only serious long-term stability problems are associated with the calibration hardware chain. An examination of engineering data for the 5 October 1993 flight (Figure 8) shows that the air temperature of the transmitter chassis varied by nearly  $10^\circ$  C during the flight. The large deviation of the transmitter base temperature is caused by instrument heating until a thermostat

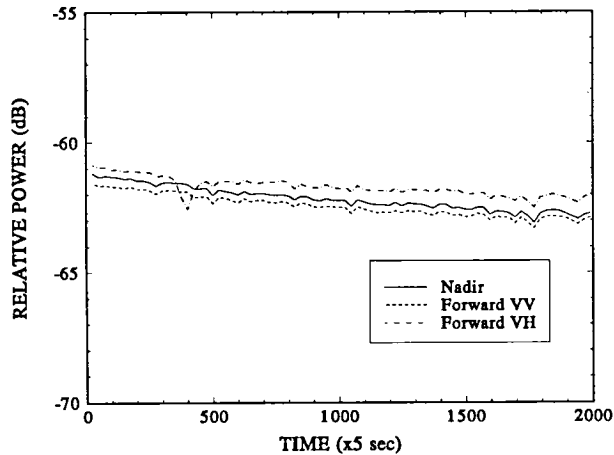


FIGURE 6. 5 October 1993 flight calibration data for the 63 dB attenuator setting.

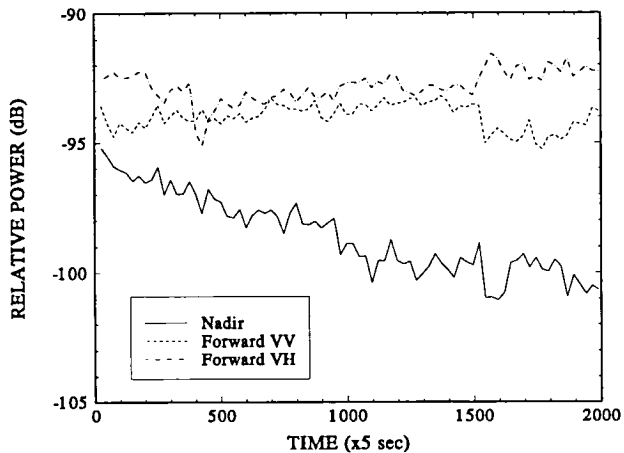


FIGURE 7. Flight calibration data for the 95 dB attenuator setting, as in Figure 6.

activates internal cooling fans.

After contacting the vendors of the various components in the calibration chain, the manufacturer of the digital attenuators acknowledged that there were known problems with temperature stability that had eventually required the units in question to be redesigned.

## 8. RANGE EQUATION

No highly accurate measurements have been made on a test range with EDOP, but analysis of the CAMEX data shows that there are no significant problems.

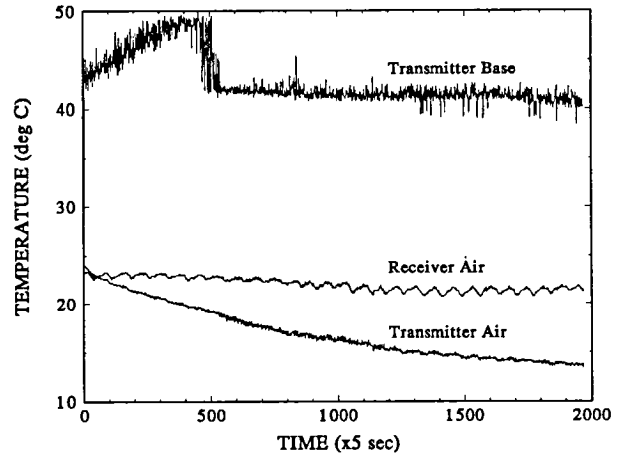


FIGURE 8. Measured temperature of the transmitter and receiver for the 5 October 1993 flight.

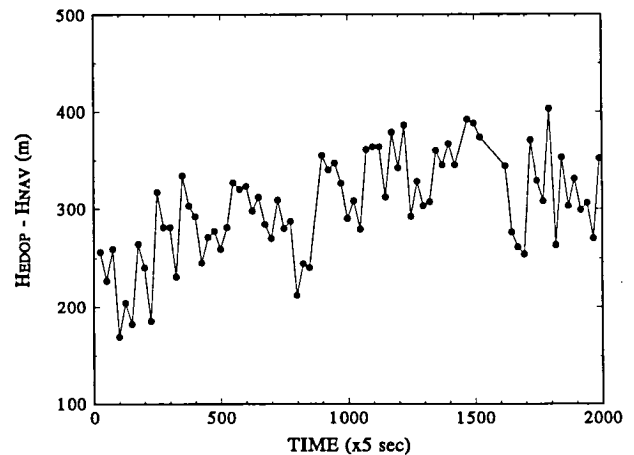


FIGURE 9. Difference between the ER-2 pressure altimeter and the derived height from EDOP reflectivity. The duration is 2.5 hours.

The timing signal which clocks the A/D converters has been measured in the laboratory. This clock, typically running at 1 MHz, has been measured to have an accuracy of better than 10 kHz. This measurement implies a gate spacing of better than 1%. Thus, for an example with a selected spacing of 150 m, each gate center is positioned to better than 1.5 m. The total cumulative error which could be introduced at a 20-km range, the nominal distance to the surface, is approximately 200 m.

The radar-derived height from the surface has also been examined. The height is determined with the following algorithm. The gates in the nadir beam containing the transmitter leakage are located. The first range gate immediately following the leakage

signal is defined as being at range zero. The gate containing the maximum surface return is then found, and the difference between gate zero and the surface gate multiplied by the gate spacing is the radar-determined aircraft altitude.

Figure 9 shows the difference in height between the radar-derived height and the ER-2 pressure altimeter. The radar-determined absolute height typically agrees to better than 400 m with the ER-2 navigation altitude. However, the magnitude of the height variations is typically less than 150 m, which is the width of one gate. It must be stressed that the ER-2 navigation system in operation during CAMEX used a pressure altitude. There is indication from other ER-2 investigators that the pressure altitude can be in error by several hundred meters and generally is an underestimate of the true aircraft height above the surface.

The height of the peak bright band signal was also determined from EDOP data for 5 October 1993. This altitude was determined by first detecting the range gate containing the maximum surface return and locating the gate with the peak bright band echo in the

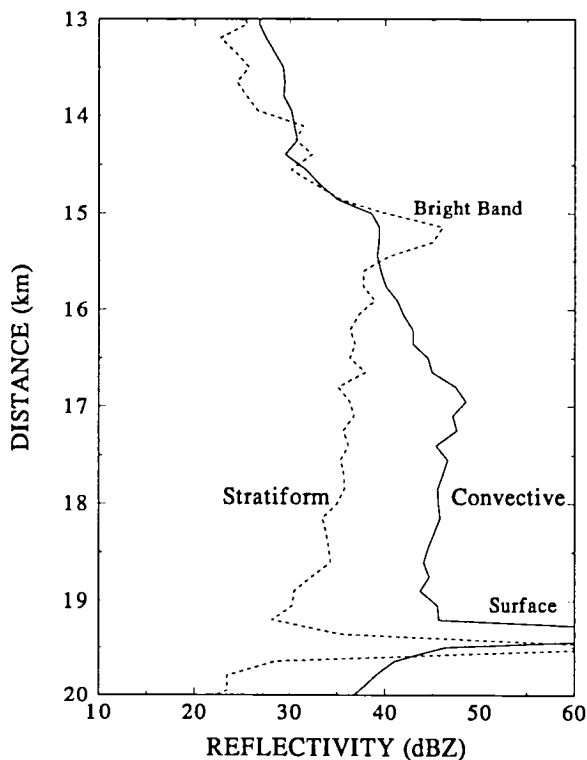


FIGURE 10. Reflectivity height profiles from the nadir antenna on 5 October 1993, showing stratiform and convective signatures.

nadir channel (Figure 10). The difference in the two gates is defined as the radar-determined bright band height, which for 5 October 1993 at 19:10 UTC was found to be approximately 4.35 km.

The 6 October 0 hr UTC radiosonde ascent from the Palm Beach National Weather Service (NWS) station showed the 0° C level to be at 4.48-km height, which is a deviation of 130 m from the EDOP observations. The radar bright band is typically found at or below the 0° C isotherm with the height depression being dependent on environmental conditions and cloud microphysics. So the EDOP ranging is consistent with external measurements and ground truth observations.

Thus, for CAMEX, the range  $R_k$  to the  $k$ th gate is

$$R_k = k\Delta R, \quad (6)$$

where  $k$  is the gate number and  $\Delta R$  is the gate spacing. During CAMEX, the gate spacing was 150 m (Table 7) and from the data set available it was not possible to verify Equation 6 for other gate spacings. It is important to emphasize that gate number  $k=0$  is defined as the first gate following the transmit pulse.

## 9. GROUND TRUTH COMPARISON

The ER-2 flew a straight-line flight track near Melbourne, Florida, on 5 October 1993. At the beginning of the track, the aircraft was approximately 280 km south of the National Weather Service (NWS) WSR-88D radar, headed north-northeast. The flight track lasted approximately 12 minutes, during which the ER-2 approached to within about 140 km of Melbourne.

As the ER-2 progressed along the track, it overflew several convective systems along a loosely arranged squall line. These observations allow for direct comparison of EDOP nadir reflectivity against a calibrated, ground-based radar. Although the large distance from Melbourne makes the WSR-88D data less than optimum, these data do provide a significant check of the EDOP calibration.

### 9.1 WSR-88D Processing

The WSR-88D is an S band coherent radar with approximately a 1° beamwidth and a range gate width of 1 km for the reflectivity scans (see Federal Meteorological Handbook No. 11). The Melbourne, Florida, WSR-88D is located at latitude 28.113056°N

and longitude 80.6544°W.

During the time of the flight track, the Melbourne radar performed three reflectivity volume scans in PPI mode. The scans were performed at 19:02:58, 19:08:54, and 19:14:51 UTC and, because of the large distances involved, only the lowest sweeps at approximately 0.44° elevation, were selected for analysis.

A special software package was written to remap the PPI scan data into geocentric coordinates of latitude and longitude. The resolution volumes (range gates) that intersected the ER-2 subtrack position were determined with an algorithm that accounts for WSR-88D beamwidth, earth curvature, and refractive bending of the beam. For each of the intersection points along the flight track, the reflectivity, coordinates and the height above the Earth's surface were determined. It is worth noting that, for a PPI scan, these data do not lie along a constant height but rather are at increasing heights as the range increases. No smoothing or averaging of the WSR-88D data was performed. A 4/3 Earth approximation was used to account for refractive effects (Doviak and Zrnic, 1984) and the radar to geocentric coordinate conversion was based upon algorithms presented by Heymsfield *et al.* (1983).

## 9.2 EDOP Processing

A comparison of EDOP and ground-based radar data presents several problems. One of those problems, as noted above, is the registration in terms of latitude and longitude of the two sets of radar data, one from a scanning ground-based radar and the other from a nadir-staring radar on a high-altitude moving platform. The coordinates for a beam of EDOP data are determined by using the latitude and longitude of the ER-2 at the point in time the EDOP dwell was collected and computing the height above ground level for each range gate in the dwell (see Section 8).

A second problem involves the differences in resolution volumes between EDOP and the WSR-88D. The WSR-88D volume is a horizontally oriented conical section 1 km long and, at the ranges of interest, several kilometers in height. In contrast, the EDOP resolution volumes are vertically oriented conical sections 150 m deep by, at most, 1 km wide at the ground. Thus, the EDOP volumes can be viewed as thin horizontal disks compared to the rather large block-shaped volumes of the WSR-88D.

The EDOP radar data were processed in such a way

that the EDOP resolution volume was roughly equivalent to the resolution volume of the WSR-88D. This was accomplished by averaging the EDOP dwells for a distance of 768 m along track. Furthermore, the vertical resolution of the EDOP data was decreased by averaging a variable number of range gates along each dwell, with the number increasing at greater distances from Melbourne. The number of gates was chosen so that the vertical-height resolution roughly matched the WSR-88D beam width at a given range.

Finally, for each of the vertically and horizontally averaged EDOP dwells, the range element was selected that was located at the height corresponding to the WSR-88D beam height above ground level.

## 9.3 Comparison of EDOP and WSR-88D

Figure 11 shows the along-track profile of the WSR-88D reflectivity (dashed line) and the EDOP reflectivity profile from the nadir antenna (solid line). During the 12 minutes required for the ER-2 to traverse the 140-km track, the Melbourne radar performed three volume scans. In order to compensate for storm movement and evolution, the WSR-88D reflectivity profile was broken into three sections, one for each of the scans. The first section at track distances 0-45 km was earliest in time (19:02:58 UTC), while the last section at 95-140 km was from the final scan at 19:14:51.

The agreement between the two profiles is slightly worse at smaller track distances, which corresponds to greater range from the Melbourne radar. This discrepancy is possibly attributed to Earth-curvature

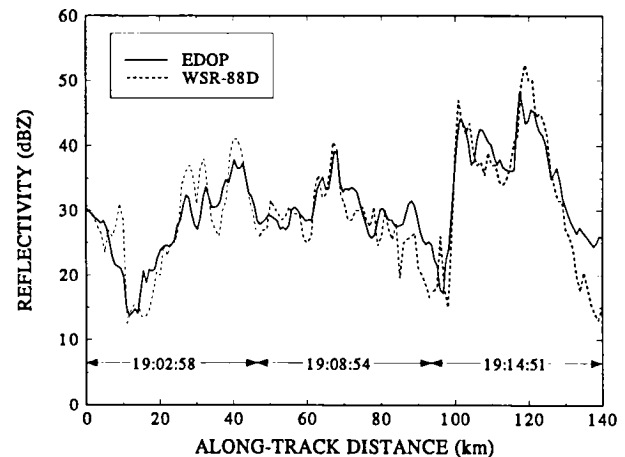


FIGURE 11. Comparison of EDOP nadir reflectivity and Melbourne, Florida, NWS WSR-88D for 5 October 1993.

and beam-bending effects that were not completely corrected with the standard atmosphere approximation (4/3 Earth-radius algorithm). Small initial errors can create relatively large displacements in the position at significant distances from the WSR-88D.

The profiles have an rms error deviation of  $\pm 6.9$  dB and there does not appear to be significant systematic bias.

## 10. OCEAN SURFACE ANALYSIS

The ocean surface presents a standard target at most microwave frequencies with the value of the scattering cross section being heavily dependent on wind speed and incidence angle of the microwaves. The wind direction and microwave polarization are smaller effects. Because the ocean surface is not a randomly distributed target which fills the complete resolution volume, a variation of the radar equation is used

$$P_r = \frac{P_t(G\lambda)^2\theta\phi I\sigma^0}{2^9\pi^2R^2\ln 2}, \quad (7)$$

where  $\sigma^0$  is the backscatter coefficient for the surface (Meneghini and Kozu, 1990). The losses are the same as those described in the previous sections.

Equation 7 describes the beam-limited case which relates the return power to the backscatter cross section when the footprint on the ocean surface is limited by the beam width. This is, in essence, a result of the pulse width (75 m for CAMEX) being relatively large for the  $3^\circ$  beam width (Nathanson, 1969; Ulaby *et al.*, 1982).

During the 5 October 1993 flight, the ER-2 performed a  $360^\circ$  turn, involving several bank angles, above a precipitation-free region of the ocean south of Florida. This turn allowed surface backscatter cross section data to be collected from the nadir beam at incidence angles of  $18^\circ$ ,  $23^\circ$ , and  $30^\circ$ . The mean and standard deviation for  $\sigma^0$  at each incidence angle were computed along a flight track distance of 12 km. Figure 12 shows the results from this surface analysis and includes a  $\sigma^0$  value for zero incidence angle which was collected when the aircraft was in level flight.

Weather buoy and ship meteorological data show that the surface winds during the 5 October 1993 flight were 3 to 7 m  $s^{-1}$ , generally in the  $60^\circ$ - $70^\circ$  direction. Representative scattering coefficients for these wind

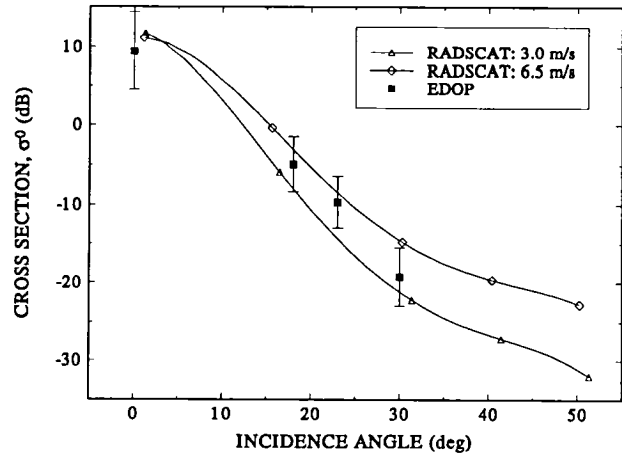


FIGURE 12. Ocean surface backscatter coefficient derived from EDOP data on 5 October 1993 (■) and NASA RADSCAT (Jones, 1977).

speeds measured with the RADSCAT  $K_u$  band scatterometer (Jones, 1977) are shown in Figure 12. In addition to wind speed, there is a lesser dependence of  $\sigma^0$  on microwave polarization and aspect angle with respect to wind direction (e.g. upwind, downwind or crosswind).

The only EDOP data available for nonzero incidence angles are from the  $360^\circ$  turn. As the  $\sigma^0$  data are computed along the 12 km segment of the turn, the aspect angle with respect to the surface wind is continuously changing. Therefore the EDOP results can be considered as an approximate mean value over aspect angle, with variation from wind direction contributing to the error bars. The deviation in  $\sigma^0$  for horizontal polarization and  $30^\circ$  incidence is approximately  $\pm 3$  dB between upwind and crosswind with the variation decreasing as the incidence angle decreases (Jones, 1977; Masuko *et al.*, 1986).

The polarization of the RADSCAT results used in Figure 12 is horizontal although there is negligible difference in the observations for polarization with incidence angles less than  $30^\circ$ . Theoretical estimates indicate that polarization differences may start to occur at incidence angles of  $20^\circ$  to  $25^\circ$  with the copolar vertical polarized returns several dB larger than for horizontal polarization (Brown, 1978). Though the polarization for EDOP is vertical with reference to the forward direction of the aircraft, as the ER-2 banks the antenna is pointed to one side of the flight track and the polarization in the plane of incidence becomes horizontal.

In general, the EDOP values are several decibels too small if the higher wind speeds are considered. Given the uncertainty in the surface wind speed at the time of observation and problems with processing the data for a single wind direction aspect angle, an adjustment to the EDOP radar constants based on these results is not considered appropriate.

## 11. FORWARD BEAM

As noted in Section 4, the forward antenna was misaligned during installation into the ER-2 for the CAMEX project, and subsequent examination of the data first showed a problem with the antenna. Although patterns of the forward antenna as used during CAMEX show degraded sidelobes and main beam, it is possible to estimate the magnitude of the problem. The results of the analysis can produce somewhat degraded reflectivity data from the forward antenna. The usefulness of the CAMEX forward antenna data will depend on the particular application.

Figure 13 shows a comparison of the nadir and forward reflectivity profiles along a 140-km track at 2.25-km height above ground (Section 9). The calibration constants derived in Section 6 were used to produce the data shown in the figure. The mean difference between the two profiles is  $5.5 \pm 3.0$  dBZ. Therefore, an increase of 5.5 dB to the forward radar constant is suggested as a suitable correction.

If the discrepancy lies solely in the antenna gain this corresponds to a 2.75-dB decrease in the gain.

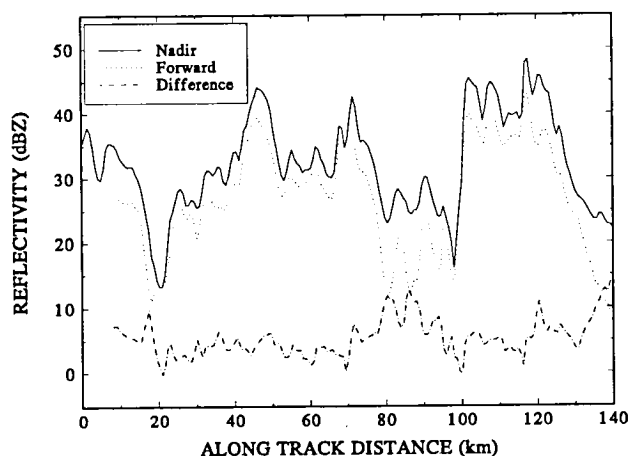


FIGURE 13. Comparison of nadir and forward reflectivity during a 140-km flight track on 5 October 1993. Height is 2.25 km above ground.

However, there is likely a degradation in the beamwidth as well.

Examination of the forward antenna cross-polar data from CAMEX show that they are corrupted most probably because of significant degradation in the cross-polar isolation of the misaligned forward antenna. As a result, no further effort has been made at this time to analyze the linear depolarization ratio (LDR) signatures obtained during CAMEX.

## 12. SUMMARY

This report presents an analysis of the calibration of the first EDOP flight data which were acquired during the 1993 CAMEX project. Previously, the radar system had been examined in the laboratory and a thermal-vacuum chamber, but during flight, the hardware experiences significantly greater thermal changes than in the laboratory. Therefore, flight data were required for a comprehensive calibration analysis.

The calibration of the EDOP receivers was accomplished from laboratory measurements, and the radar constants were computed. Using this calibration, the radar reflectivity was estimated for the CAMEX data set. Comparison of these data with ground truth provided by a NWS WSR-88D radar show good agreement with EDOP nadir reflectivity and an rms error of approximately  $\pm 6.9$  dBZ. The results of an analysis of the backscatter cross section from the ocean surface also agree to better than 3 dB with published scatterometer results. Although these two numbers are moderately large, they represent deviations from other observations rather than errors in EDOP calibration. The EDOP absolute calibration is considered to be significantly better than 3 dB.

Analysis of height data shows no problems with ranging of the EDOP data. After an initial period of 30 to 40 minutes, which is required to reach thermal equilibrium, the microwave transmitter and receiver, excluding the calibration chain, appear to be stable to better than 0.25 dB during flight.

Through analysis of the CAMEX data and subsequent laboratory tests, several problems were pinpointed with the hardware. Results indicated that the radar constant for the forward antenna should be increased by 5.5 dB for the CAMEX observations to compensate for problems in the antenna alignment. A realignment of the forward antenna has been successfully completed by GSFC personnel, and the resulting

patterns closely match the original specification. GSFC engineering staff are modifying the calibration chain for improved temperature stability and will tune the signal conditioning electronics prior to the next campaign in order to bring the IF amplifier into dynamic range of the digital converter.

Although difficult, at some stage a complete end-to-end calibration including antennas should be performed. Given the difficulties of using a balloon-borne sphere target, another option would be to operate EDOP from the ground near a calibrated ground-based radar, which would allow comparison of reflectivity profiles.

For future campaigns, a number of recommendations are put forward which will aid the accuracy of the reflectivity calibration and its ease of implementation.

- A standard procedure for calibration should be defined. In particular, the procedure should account for hardware configuration such as variable PRF, pulse width, and IF filters.
- A standard calibration should be performed immediately before and after a campaign to provide a performance base line. The calibration should preferably be performed with the hardware in flight configuration.
- Efforts should be made to obtain ground truth for precipitation reflectivity, over a calibrated radar, at least once during each campaign.
- A series of banking maneuvers should be performed over a cloud-free area of the ocean to collect surface backscatter data for calibration comparisons. This procedure should be done at the end of a flight so that the system has thermally stabilized.

### 13. REFERENCES

Brown, G.S., 1978: Backscattering from a Gaussian-distributed perfectly conducting rough surface. *IEEE Trans. Antennas Propagat.*, **AP-26**, 472-482.

Davis, I., 1991: *ER-2 Aircraft Doppler Radar (EDOP) Antenna System*, ERA Report No. 91-0261, ERA Technology Ltd., Cleeve Road Leatherhead, Surrey KT22 7SA, England.

Dicaudo, V.J., 1970: Radomes. *Radar Handbook*, M.I. Skolnik, ed., McGraw-Hill: New York., 14.1-14.15.

Doviak, R.J., and D.S. Zrnic, 1979: Receiver bandwidth effect on reflectivity and Doppler velocity estimates. *J. Appl. Meteor.*, **18**, 69-76.

Doviak, R.J., and D.S. Zrnic, 1984: *Doppler Radar and Weather Observations*. Academic Press: New York, Chap. 2.

Heymsfield, G.M., W. Boncyk, S. Bidwell, D. Vandemark, S. Ameen, S. Nicholson, and L. Miller, 1993: Status of the NASA/EDOP airborne radar system. *26th International Conf. Radar Meteorology*, Norman, Amer. Meteor. Soc., 374-375.

Heymsfield, G.M., L.R. Dod, L. Miller, M. Craner, and D. Vandemark, 1991: Update on the NASA ER-2 Doppler radar system (EDOP). *25th International Conf. Radar Meteorology*, Paris, Amer. Meteor. Soc., 855-858.

Heymsfield, G.M., K.K. Ghosh, and L.C. Chen, 1983: An interactive system for compositing digital radar and satellite data. *J. Climate Appl. Meteor.*, **22**, 705-713.

Heymsfield, G.M., C. Parsons, L.R. Dod, and L. Miller, 1989: Planned ER-2 Doppler radar (EDOP) for studying convective storms and mesoscale phenomena. *24th International Conf. Radar Meteorology*, Tallahassee, Amer. Meteor. Soc., 581-584.

Jones, W.L., L.C. Schroeder, and J.L. Mitchell, 1977: Aircraft measurements of the microwave scattering signature of the ocean. *IEEE Trans. Antennas Propagat.*, **AP-25**, 52-61.

Masuko, H., K. Okamoto, M. Shimada, S. Niwa, 1986: Measurement of microwave backscattering signatures of the ocean surface using X band and K<sub>a</sub> band airborne scatterometers. *J. Geophys. Res.*, **91** (C11), 13065-13083.

Meneghini, R., and T. Kozu, 1990: *Spaceborne Weather Radar*. Artech House: Norwood, MA, 199 pp.

Nathanson, F.E., 1969: *Radar Design Principles*. McGraw-Hill: New York.

Office of the Federal Coordinator for Meteorological Services and Supporting Research, 1991: *Federal Meteorological Handbook No. 11: Doppler Radar Meteorological Observations*. U.S. Department of Commerce, FCM-H11.

Ulaby, F.T., R.K. Moore, and A.K. Fung: 1982: *Microwave Remote Sensing*. Addison-Wesley: Reading, MA, Volume II.

Zrnic, D.S., 1975: Moments of estimated input power for finite sample averages of radar receiver outputs. *IEEE Trans. Aerospace Elec. Syst.*, **AES-11**, 109-113.

REPORT DOCUMENTATION PAGE			Form Approved OMB No. 0704-0188	
Public reporting burden for this collection of information is estimated to average 1 hour per response, including the time for reviewing instructions, searching existing data sources, gathering and maintaining the data needed, and completing and reviewing the collection of information. Send comments regarding this burden estimate or any other aspect of this collection of information, including suggestions for reducing this burden, to Washington Headquarters Services, Directorate for Information Operations and Reports, 1215 Jefferson Davis Highway, Suite 1204, Arlington, VA 22202-4302, and to the Office of Management and Budget, Paperwork Reduction Project (0704-0188), Washington, DC 20503.				
1. AGENCY USE ONLY (Leave blank)	2. REPORT DATE August 1994	3. REPORT TYPE AND DATES COVERED Technical Memorandum		
4. TITLE AND SUBTITLE NASA ER-2 Doppler Radar Reflectivity Calibration for the CAMEX Project			5. FUNDING NUMBERS  912	
6. AUTHOR(S)  I. J. Caylor, G. M. Heymsfield, S. W. Bidwell, and S. Ameen				
7. PERFORMING ORGANIZATION NAME(S) AND ADDRESS (ES)  Goddard Space Flight Center Greenbelt, Maryland 20771			8. PERFORMING ORGANIZATION REPORT NUMBER  94B00110  Code 912	
9. SPONSORING / MONITORING AGENCY NAME(S) AND ADDRESS (ES)  National Aeronautics and Space Administration Washington, DC 20546-0001			10. SPONSORING / MONITORING AGENCY REPORT NUMBER  NASA TM-104611	
11. SUPPLEMENTARY NOTES J. Caylor and S. Ameen: Science Systems and Applications, Inc., Lanham, Maryland (located at Goddard Space Flight Center, Greenbelt, Maryland); G. Heymsfield and S. Bidwell, Goddard Space Flight Center, Greenbelt, Maryland				
12a. DISTRIBUTION / AVAILABILITY STATEMENT Unclassified - Unlimited Subject Category 47 This publication is available from the NASA Center for AeroSpace Information, 800 Elkridge Landing Road, Linthicum Heights, MD 21090-2934, (301)621-0390.			12b. DISTRIBUTION CODE	
13. ABSTRACT (Maximum 200 words)  The NASA ER-2 Doppler radar (EDOP) was flown aboard the ER-2 high-altitude aircraft in September and October 1993 for the Convection and Moisture Experiment. During these flights, the first reliable reflectivity observations were performed with the EDOP instrument. This report details the procedure used to convert real-time engineering data into calibrated radar reflectivity. Application of the calibration results produces good agreement between the EDOP nadir pointing reflectivity and ground truth provided by a National Weather Service WSR-88D radar. The rms deviation between WSR-88D and EDOP is 6.9 dB, while measurements of the ocean surface backscatter coefficient are less than 3 dB from reported scatterometer coefficients. After an initial 30-minute period required for the instrument to reach thermal equilibrium, the radar is stable to better than 0.25 dB during flight. The range performance of EDOP shows excellent agreement with aircraft altimeter and meteorological sounding data.				
14. SUBJECT TERMS Precipitation radars; radar calibration; CAMEX; EDOP, radar equation; surface reference, ground truth - WSR-88D; remote sensing; and precipitation			15. NUMBER OF PAGES 24	
			16. PRICE CODE	
17. SECURITY CLASSIFICATION OF REPORT Unclassified	18. SECURITY CLASSIFICATION OF THIS PAGE Unclassified	19. SECURITY CLASSIFICATION OF ABSTRACT Unclassified	20. LIMITATION OF ABSTRACT UL	



National Aeronautics and  
Space Administration  
**Goddard Space Flight Center**  
Greenbelt, Maryland 20771

Official Business  
Penalty for Private Use, \$300



SPECIAL FOURTH-CLASS RATE  
POSTAGE & FEES PAID  
NASA  
PERMIT No. G27



POSTMASTER: If Undeliverable (Section 158,  
Postal Manual) Do Not Return

---